A nontransgenic mouse model shows inducible amyloid-β (Aβ) peptide deposition and elucidates the role of apolipoprotein E in the amyloid cascade

Iftach Dolev and Daniel M. Michaelson*

Department of Neurobiochemistry, The George S. Wise Faculty of Life Sciences, Tel Aviv University, 69978 Tel Aviv, Israel

Edited by Eugene Roberts, Beckman Research Institute of the City of Hope, Duarte, CA, and approved August 4, 2004 (received for review June 22, 2004)

The amyloid-β (Aβ) peptide, a major pathological hallmark of Alzheimer's disease (AD), undergoes a cascade of interactions resulting in the formation of soluble aggregates and their conversion in the brain to insoluble deposits and mature senile plaques. Furthermore, the apoE4 isoform of apolipoprotein E (apoE), which is the major genetic risk factor of AD, is associated with increased Aβ deposition. It is not known how the different Aβ aggregates in the amyloid cascade are formed, contribute to the pathogenesis of AD, or are affected by apoE4. To investigate the initial aggregation stages underlying the amyloid cascade *in vivo* and how apoE affects them, we examined the effects of prolonged inhibition and subsequent reactivation of the Aβ-degrading protease neprilysin on deposition, disaggregation, and fibrillization of Aβ in apoE-transgenic and control mice. In control mice, intracerebroventricular infusion of thiorphan, which inhibits neprilysin, induced Aβ42 and Aβ40 deposition and fibrillization. On termination of thiorphan treatment, the number of Aβ deposits decreased, whereas the fibrillar Aβ deposits were unaffected. Similar treatments in apoE-deficient mice and mice transgenic for human apoE4 or apoE3 revealed that apoE4 enhances specifically the nucleation and aggregation of immunopositive Aβ deposits and that reversible disaggregation of these deposits and their irreversible conversion to fibrillar deposits are stimulated similarly by the different apoE isoforms. Deposition of Aβ and its enhancement by apoE4 were accompanied by increased astrogliosis both far from and near the Aβ deposits, suggesting that astrogliosis might be triggered by both insoluble and soluble Aβ aggregates.

Converging genetic and histopathological observations led to the formulation of the amyloid hypothesis, which proposes that accumulation of amyloid-β (Aβ) peptide, a major constituent of the brain plaques characteristic of Alzheimer's disease (AD), is the primary event in AD pathogenesis (1, 2). Recent findings suggest that brains of individuals with AD also contain soluble and neurotoxic Aβ oligomers, which seem to be an intermediate state in the Aβ-aggregation cascade, whose downstream product is the senile plaque (3–10). There is poor correlation between the severity of dementia and the density of amyloid plaques in AD (11–13); furthermore, in mice transgenic for the human Aβ precursor protein (APP), synaptic degeneration and cognitive decline are observed even before amyloid is deposited (14–16). This finding suggests that the pathological effects of Aβ in AD are mediated by Aβ aggregates that precede the formation of the senile plaque. The relative contributions of the different soluble and insoluble Aβ aggregates to the pathology of AD and the mechanisms underlying their formation *in vivo* are not yet known.

Apolipoprotein E (apoE), the major brain lipid-binding protein, is expressed in humans as three isoforms (apoE2, apoE3, and apoE4), which differ in one or two amino acids (17). The apoE4 genotype is the major genetic risk factor for AD, and the age at disease onset is inversely related to its gene dosage (18–20). Furthermore, senile plaques contain apoE, and the gene dose of the apoE4 allele in AD correlates positively with increased Aβ deposition (21). Studies using APP- and apoE-transgenic mice indicated that apoE enhances Aβ deposition and is required for fibrillization (22–24) and that these effects are significantly more pronounced in aged apoE4 transgenic mice than in their counterparts that express the AD-benign allele apoE3 (23–25). These observations point to direct isoform-specific involvement of apoE in the Aβ cascade. However, the usefulness of APP- and apoE-transgenic mice in studying the Aβ-aggregation cascade and how apoE4 affects it are limited by the slow and asynchronous deposition of Aβ that evolves in these mice over many months.

Neprilysin, insulin-degrading enzyme, and endothelin-converting enzyme all play a role in the catabolism of Aβ *in vivo*, and mice deficient in these proteases exhibit elevated Aβ levels (26–29). Furthermore, overexpression of neprilysin in APP-transgenic mice reduces Aβ deposition (30, 31). Synthetic Aβ injected into the mouse brain undergoes rapid degradation, which is blocked by the neprilysin inhibitor thiorphan (26). Moreover, most of the Aβ remains intact when injected into neprilysin-deficient mice (27), suggesting that steady-state levels of Aβ are strongly affected by neprilysin and that this enzyme degrades extracellular Aβ.

Here, we studied the mechanisms underlying the deposition of Aβ *in vivo* and the isoform-specific effects thereon of apoE. We conducted this study by inducing prolonged inhibition of neprilysin in the brains of apoE-transgenic and control mice and determining the effects on Aβ deposition. The results indicated that apoE4 stimulates, in an isoform-specific fashion, the nucleation and aggregation of Aβ deposits and that reversible disaggregation of these deposits and their irreversible conversion to fibrillar deposits are stimulated by apoE and are affected similarly by the different apoE isoforms.

Materials and Methods

Transgenic Mice. Human apoE3- and apoE4-transgenic mice, generated on an apoE-deficient C57BL/6J background by using human apoE3- and apoE4-transgenic constructs (32), were obtained from A. Roses (Duke University, Durham, NC). The mice used in our experiments were from lineages apoE3-453 and apoE4-81, which express similar levels of brain apoE (33). ApoE-transgenic mice were backbred with genetically homogeneous apoE-deficient mice (The Jackson Laboratory, catalog no. N10 JAX) for >10 generations and were heterozygous for the human apoE transgene and homozygous for mouse apoE deficiency. The apoE genotype of the mice was confirmed by PCR analysis, as described in ref. 34.

Mice (5-month-old males) were divided into groups bearing either the human apoE3 or apoE4 transgene. A third and fourth group comprised, respectively, apoE-deficient mice that were pooled siblings of these transgenic mice (35) and C57BL/65 controls. All experiments were approved by the Tel Aviv University Animal Care Committee, and every effort was made to reduce animal stress and to minimize animal usage.

This paper was submitted directly (Track II) to the PNAS office.

Abbreviations: Aβ, amyloid-β; AD, Alzheimer's disease; apoE, apolipoprotein E; APP, amyloid precursor protein; i.c.v., intracerebroventricular.

*To whom correspondence should be addressed. E-mail: dmichael@post.tau.ac.il.

Implantation of Alzet Miniosmotic Pumps. Alzet miniosmotic pumps (model 2004, Alzet, Palo Alto, CA), which deliver their contents at a rate of 0.25 μl/h for up to 1 month, were each connected by means of a polyethylene catheter to a stainless steel cannula (Brain Infusion kit, Alzet) and loaded either with 0.5 mM thiorphan (Sigma) in artificial cerebrospinal fluid containing 1 mM ascorbic acid (26) or with a similar solution without thiorphan. Mice were anesthetized by i.p. injection of ketamine (120 mg/kg), their skulls were carefully exposed, and a small hole was drilled with a 25-gauge needle above the lateral ventricle (1 mm posterior and 1.5 mm lateral to the bregma). The tip of the brain infusion cannula was inserted into the hole, and the cannula was glued to the skull (Luctite 454). To complete the procedure, the pump was inserted s.c. on the mouse's back, and the cut skin over the skull was sutured. An antibiotic (1% oxytetracycline) was added to the drinking water for 1 week. For Aβ-deposition experiments, mice were kept for up to 4 weeks after the pumps were implanted. To assess the reversibility of Aβ deposits, pumps were retained in the mice for 4 weeks and then removed, and the tubing connecting them to the cannula was disconnected and sealed. The mice were then kept for an additional 8 weeks before being examined.

Immunohistochemistry and Histochemistry. ApoE3-transgenic, apoE4-transgenic, apoE-deficient, and control mice, all treated with thiorphan for the indicated periods, and corresponding sham-treated and naïve mice were anesthetized with ketamine (120 mg/kg i.p.), perfused transcardially with PBS, and fixed with 4% formaldehyde in PBS. Brains were removed and postfixed overnight in fixative solution, immersed for cryoprotection in 30% sucrose for 24 h at 4°C, and frozen in tissue-freezing medium (Jung, Leica, Deerfield, IL). Frozen brain coronal sections (10 μm) were cut and stained immunohistochemically as described in ref. 34. Sections were viewed and photographed at $\times$40 magnification by using a Supercam camera (Applitec, Holon, Israel). The following primary antibodies were used: mAbs G211 and G210 (dilution 1:1,000) specific to Aβ42 and Aβ40, respectively (36), a gift from T. Hartmann (Heidelberg University, Heidelberg); mAb 4G8 (dilution 1:2,000; Chemicon), which binds to both Aβ40 and Aβ42; FC3340 rabbit anti-Aβ40 and FC3542 rabbit anti-Aβ42 antisera (dilution 1:1,000), gifts from F. Checler (Centre National de la Recherche Scientifique, Valbonne, France); mAb22C11 (dilution 1:1,000; Chemicon) specific to APP; goat anti-human apoE (dilution 1:5,000; Chemicon); rabbit anti-neprilysin (dilution 1:2,000; Chemicon); and anti-glial fibrillary acidic protein mAb (dilution 1:50; DAKO). Sections were double-labeled in the same way, except that the primary antibodies used were from different hosts, and their corresponding second antibodies were tagged with distinct fluorescent labels.

Fibrillar Aβ depositions were visualized by fluorescence imaging using thioflavin-S. To this end, staining with Mayer's hematoxylin was followed by incubation with 1% thioflavin-S (Sigma) in water for 4 min. Slides were then immersed in 1% acetic acid for 20 min and covered with antifade mounting medium (ImmunoGlo).

Numbers and sizes of the Aβ deposits were determined by using coded sections and the IMAGE-PRO PLUS program (Media Cybernetics, Silver Spring, MD). The program was set to detect objects with an intensity at least 3-fold higher than background and a size $<$150 μm and $>$6 μm. Some sections also were counted directly, and results obtained by the two methods deviated by $<$10%. The total number of Aβ deposits corresponds to the immunopositive Aβ40 or Aβ42 deposits, whereas the number of fibrillar deposits corresponds to the thioflavin-S positive deposits. The size of a deposit was determined by delineating its perimeter manually and by using the program to calculate the engulfed area.

Immunoblot Assays. Brain slices from the area enriched in Aβ deposits ($-$1.5 to $-$3.5 mm from bregma) were homogenized in 100 mM sodium carbonate buffer (pH 11.5). The homogenate was centrifuged (100,000 $\times$ *g* for 30 min), and the insoluble Aβ-containing pellet was extracted with guanidine·HCl and sonicated for 10 min as described in ref. 37. The soluble and the resuspended insoluble Aβ were blotted and immunoreacted with mAb 4G8, which recognizes both Aβ40 and Aβ42 (37), after which they were quantified by using mouse Aβ40 standards and computerized densitometry (33).

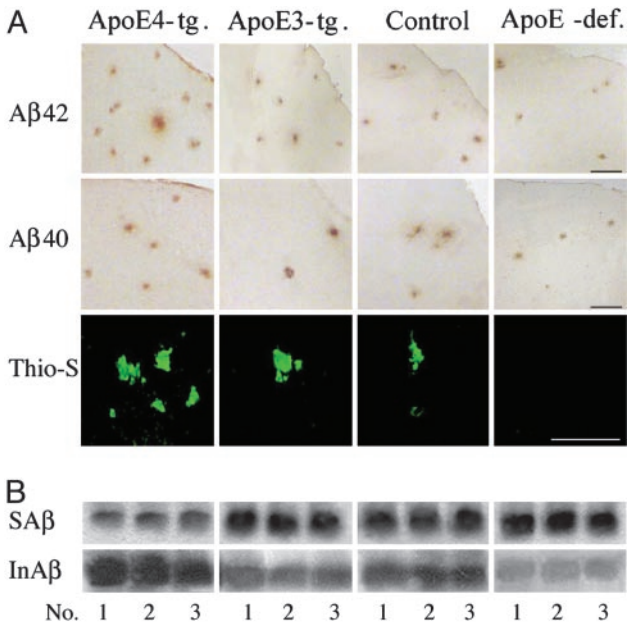

Fig. 1. Effects of the apoE genotype on Aβ deposition after inhibition of neprilysin. (*A*) Representative micrographs of cortical fields of coronal brain sections (bregma $-$2.8 mm) from apoE4- (ApoE4-tg.) and apoE3- (ApoE3-tg.) transgenic, apoE-deficient (ApoE-def.), and control mice infused i.c.v. for 1 month with the neprilysin inhibitor thiorphan (see *Materials and Methods*). (*B*) Representative immunoblots of soluble (SAβ) and insoluble (InAβ) Aβ of the same groups of three mice each. Immunohistochemistry (anti-Aβ42 mAb G211 and anti Aβ40 mAb G210), histochemistry (thioflavin-S), and immunoblot analysis (anti-Aβ mAb 4G8) were performed as described in *Materials and Methods*. (Scale bar, 50 μm.)

Statistical Analysis. Numbers and sizes of Aβ deposits are expressed as means $\pm$ SD. Differences among means of the experimental groups and their distinct parameter interactions were analyzed either by repeated-measures ANOVA (Fig. 2), with genotype and brain sections as independent factors, or by one-way and two-way ANOVA (Figs. 3, 4, and 6) with genotype and treatment as independent factors. When ANOVA indicated a significant difference between groups, Tukey's test was used for post hoc comparisons of results.

Results

Intracerebroventricular (i.c.v.) infusion of the neprilysin inhibitor thiorphan into apoE3- and apoE4-transgenic, control, and apoE-deficient mice, by an Alzet miniosmotic pump for 1 month, resulted in formation of Aβ42 and Aβ40 deposits that were most dense in apoE4-transgenic mice (Fig. 1*A*). Both apoE3- and apoE4-containing transgenic mice, as well as the control group, also had thioflavin-S-positive fibrillar Aβ deposits, which were most dense in apoE4-transgenic mice, whereas no fibrillar Aβ deposits were detectable in apoE-deficient mice (Fig. 1*A*). No fibrillar Aβ or immunopositive deposits were observed in any of the sham-injected mice (data not shown).

The effects of apoE on formation of Aβ42, Aβ40, and fibrillar Aβ deposits were determined quantitatively first by rostrocaudal measurements of their numbers in coronal sections from bregma $-$4 to

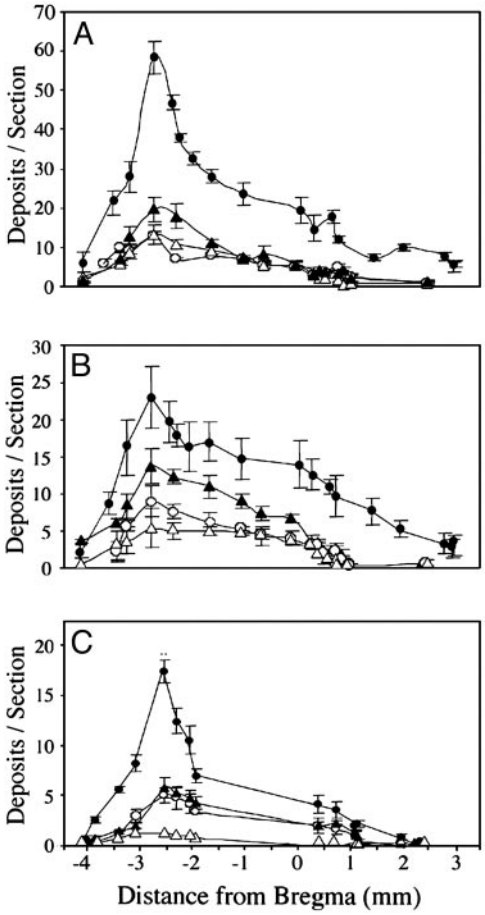

Fig. 2. Rostrocaudal distribution of Aβ42 (*A*), Aβ40 (*B*), and fibrillar Aβ (*C*) deposits in brains of apoE-transgenic and control mice after inhibition of neprilysin. ApoE4-transgenic (●), apoE3-transgenic (○), apoE-deficient (△), and control (▲) mice were infused i.c.v. with thiorphan for 1 month (see *Materials and Methods*). Brains were then cut coronally (−4 mm to +3 mm from bregma), and consecutive coronal sections at the indicated positions were stained for Aβ42 (mAb G211), Aβ40 (mAb G210), or fibrillar Aβ deposits (thioflavin-S) (see *Materials and Methods*). Values (means ± SD of four or five mice per group) are for two sections per mouse at each of the indicated bregma levels.

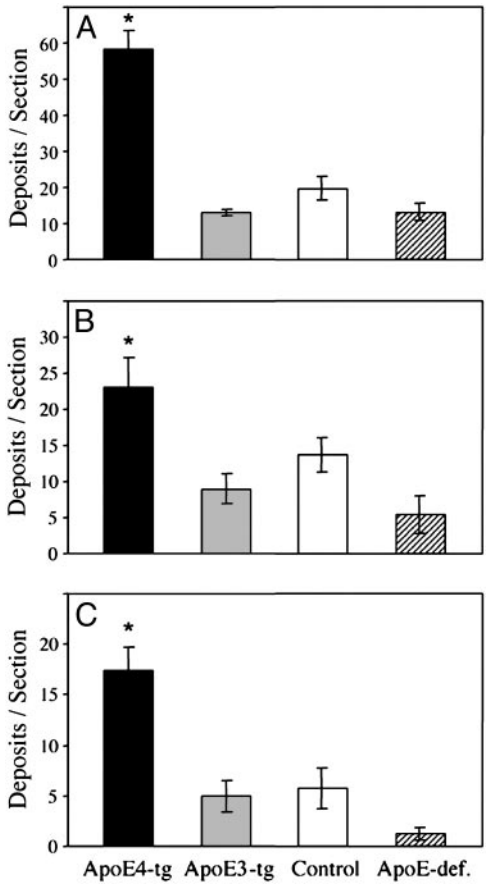

Fig. 3. Quantitative determination of the numbers of Aβ42 (*A*), Aβ40 (*B*), and fibrillar Aβ (*C*) deposits in brains of apoE4-transgenic (ApoE4-tg), apoE3-transgenic (ApoE3-tg), apoE-deficient (ApoE-def.), and control mice after i.c.v. infusion of thiorphan for 1 month (see *Materials and Methods*). Coronal sections at the level of maximal Aβ deposition (bregma −2.8) were stained with anti-Aβ42 (mAb G211) or anti-Aβ40 (mAb G210) antibodies or with thioflavin-S (see *Materials and Methods*). Values (means ± SD of four or five mice per group) for each of the Aβ deposition measurements are for two sections per mouse. *, $P < 0.001$ for the total number of Aβ42, Aβ40, and fibrillar Aβ deposits of apoE4 transgenic mice relative to those of the other mouse groups.

+3 mm. In all brain sections examined, immunohistochemically detectable and thioflavin-S-positive Aβ deposits in the apoE4 mice were more abundant than the corresponding Aβ deposits in the other groups, and the numbers of these deposits in each of the groups were maximal at bregma −2.8 mm (Fig. 2). ANOVA plus repeated-measurement analysis indicated a significant effect of "mouse group × brain area" on Aβ42, Aβ40, and fibrillar Aβ deposition ($P < 0.001$). This rostrocaudal distribution of the density of Aβ deposits is similar to that of the size of the surface area of the lateral vesicle into which thiorphan was injected (38), suggesting that the spatial distribution of Aβ deposits in the brain reflects the diffusion and resulting distribution of i.c.v.-infused thiorphan in the brain. The effects of apoE on Aβ deposition were compared quantitatively on coronal sections, in which Aβ deposition was maximal for all groups (bregma −2.8 mm). The comparison indicated that the numbers of Aβ42, Aβ40, and fibrillar Aβ deposits in apoE4 mice (respectively 58 ± 8, 23 ± 8, and 17 ± 2 deposits per section) were 3- to 4-fold higher than those of apoE3 mice (Fig. 3). One-way ANOVA of these results revealed a significant effect of group for the three measurements of Aβ deposition ($P < 0.001$), which was associated with significantly larger numbers of Aβ42, Aβ40, and fibrillar Aβ deposits in the apoE4-transgenic mice than in the other groups ($P < 0.05$). Similar results were obtained with the Aβ42 and Aβ40 antisera FC3542 and FC3340 and with mAb 4G8. Furthermore, the deposits did not react with anti-APP mAb 22C11 (data not shown). Control immunoblot experiments using mAb 4G8 indicated that the amounts of insoluble Aβ in apoE4 mice (25 ± 4 pg/mg tissue) were larger than those of the apoE3, control, and apoE-deficient mice (respectively 9 ± 0.3, 10 ± 0.8, and 7.5 ± 0.3 pg/mg tissue) in the other groups and that this increase was accompanied by a compensatory decrease in soluble Aβ of the apoE4 (8 ± 0.3 pg/mg tissue) relative to those of apoE3, control, and apoE-deficient mice (respectively 10 ± 1, 10 ± 1, and 10 ± 0.9 pg/mg tissue) (Fig. 1*B*). Additional immunohistochemical controls indicated that the amounts of neprilysin in the four groups were similar before and after thiorphan treatment (data not shown).

Kinetic analysis of Aβ deposition disclosed a progressive increase in each of the groups for at least 4 weeks, except for the lack of fibrillar Aβ deposition in apoE-deficient mice (Fig. 4). Two-way ANOVA of these results revealed a significant effect of "mouse group × time" for mouse Aβ42, Aβ40, and fibrillar Aβ deposits ($P < 0.001$), which was associated with significantly larger numbers of Aβ42 and Aβ40 deposits, at both 2 and 4 weeks of treatment, in the apoE4 mice than in the other groups, with a corresponding

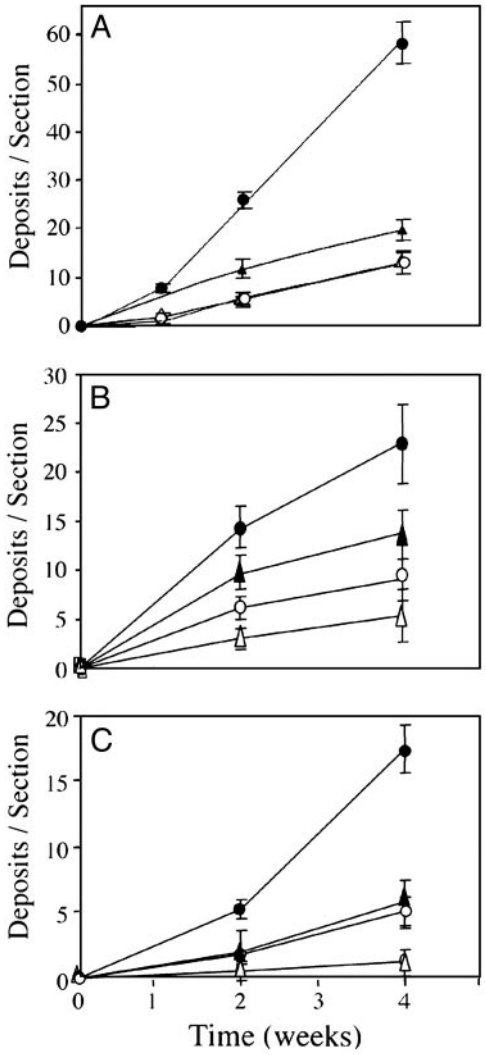

Fig. 4. Kinetics of deposition of Aβ42 (*A*), Aβ40 (*B*), and fibrillar Aβ (*C*) in the brains of apoE4-transgenic (●), apoE3-transgenic (○), apoE-deficient (△), and control (▲) mice. Mice were infused i.c.v. with thiorphan (see *Materials and Methods*) for the indicated times, after which their brains were excised, and coronal sections (bregma −2.8 mm) were stained for Aβ42 (*A*), Aβ40 (*B*), or fibrillar Aβ (*C*) (see *Materials and Methods*). Values (means ± SD) for Aβ42, Aβ40, and fibrillar Aβ deposition each correspond to two sections per mouse of four or five mice per "group × time point."

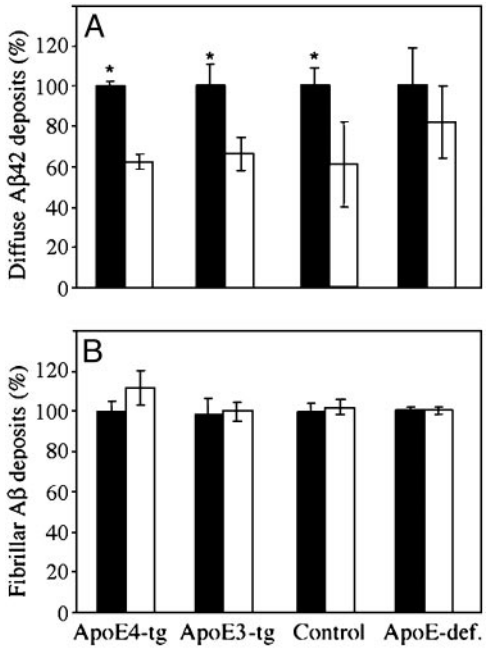

Fig. 5. Effect of the apoE genotype on disaggregation of Aβ42 deposits (*A*) and fibrillar Aβ deposits (*B*) after removal of thiorphan. ApoE4 (ApoE4-tg), apoE3 (ApoE3-tg), apoE-deficient (ApoE-def.), and control mice were injected i.c.v. with thiorphan (see *Materials and Methods*) for 1 month. The mice were then killed either immediately or 8 weeks later. Values (means ± SD) of Aβ42 and fibrillar Aβ deposits per coronal section (bregma −2.8) are for four or five mice per "group × time." White bars represent the percentage of Aβ42 and fibrillar Aβ deposits observed in each group 8 weeks after termination of thiorphan treatment, relative to their corresponding levels immediately after termination of thiorphan treatment (black bars). *, $P < 0.001$.

significant increase in the numbers of fibrillar Aβ deposits in apoE4 mice at 4 weeks ($P < 0.05$).

To determine the extent to which Aβ deposition is reversible, we measured the deposits after termination of the thiorphan treatment (Fig. 5). Deposits of Aβ42 were significantly decreased 8 weeks after thiorphan was removed ($P < 0.001$ for "group × treatment"; two-way ANOVA); this effect was accompanied by a significant decrease (≈35%) in Aβ42 deposits of control, apoE4, and apoE3 mouse groups ($P < 0.002$), but with no significant change in the corresponding Aβ42 deposits of apoE-deficient mice. In contrast, numbers of fibrillar Aβ deposits did not change in any of the groups during this period. These findings indicate that the deposition of Aβ42 is reversible and suggest that its disaggregation is enhanced by apoE, but not in an isoform-specific fashion. In contrast, within the time scale of the experiment, the fibrillization of Aβ was found to be irreversible.

Analysis of the size distribution of Aβ42 deposits disclosed the presence of a major population (≈85%) of small deposits whose sizes were similar in the four groups (diameters of 8 ± 1.7 μm) and did not change between the 2- and 4-week time points, as well as a subpopulation of larger Aβ42 deposits (see example in Fig. 1*A Top Left*), whose diameters increased similarly in all of the groups, from 38 ± 7 μm at 2 weeks to 56 ± 3 μm at 4 weeks. Similar results were obtained for Aβ40 deposits, except that they were ≈2-fold larger than the corresponding Aβ42 deposits. These findings suggest that, unlike the isoform-specific effects of apoE4 on nucleation and deposition of Aβ42 and Aβ40, the effects of apoE4 on the size and growth of these deposits are not specific to a particular isoform. Double-labeling experiments indicated that >85% of the Aβ42- and Aβ40-positive deposits of apoE-containing mice also stained positively for apoE (data not shown).

The extent to which thiorphan-induced deposition of Aβ is associated with brain neuropathology was investigated immunohistochemically, by using the astrocytic marker glial fibrillary acidic protein, 4 weeks after initiation of thiorphan treatment. This investigation revealed that thiorphan induced astrocytic activation in the vicinity of Aβ deposits and in Aβ-free areas. The former were prominent in the cortex (Fig. 6 *A* and *B*), whereas astrogliosis spatially dissociated from the Aβ deposits was particularly abundant in the hippocampus (Fig. 6 *C* and *D*). Activated astrocytes associated with Aβ deposits were more numerous in apoE4-transgenic mice than in other groups, in accordance with the demonstration of the largest numbers of Aβ deposits in these mice (Fig. 3). In contrast, numbers of activated astrocytes that were spatially dissociated from the Aβ deposits were similar in all apoE-containing mice, but were lower in apoE-deficient mice.

Discussion

The results of this study indicated that deposition of Aβ *in vivo* is initiated by reversible aggregation of Aβ that subsequently under-

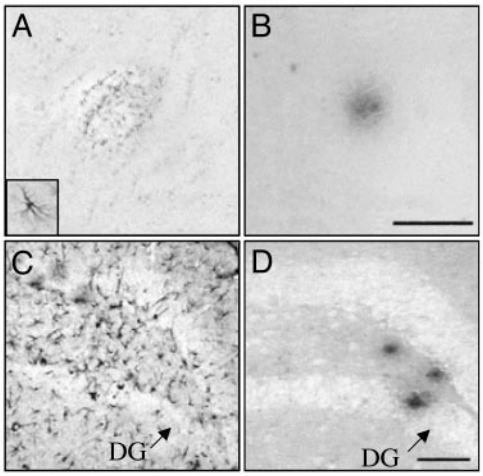

Fig. 6. Effects of inhibition of neprilysin on astrogliosis. Micrographs show representative consecutive cortical (*A* and *B*) and hippocampal (*C* and *D*) sections from an apoE4-transgenic mouse treated for 1 month with thiorphan (see *Materials and Methods*) (*A Inset*) An activated astrocyte (×5 relative to *A*). *A* and *C* were labeled with anti-glial fibrillary acidic protein mAbs, and *B* and *D* were labeled with the anti-Aβ42 mAb G211. DG, dentate gyrus. (Scale bars, 50 μm.)

goes irreversible fibrillization and that these processes are affected differentially and in an isoform-specific fashion by apoE (shown schematically in Fig. 7). Immunopositive Aβ deposits were significantly more abundant in apoE4-transgenic mice than in apoE3-transgenic, apoE-deficient, or control mice, in all of which the corresponding numbers of Aβ deposits were similar (Figs. 1 and 2). In contrast, both the extent of disaggregation of the Aβ deposits and their fibrillization were similar in apoE4-transgenic mice and controls and were insignificant in apoE-deficient mice. These findings suggest that apoE4 stimulates the nucleation and aggregation of Aβ in an isoform-specific fashion and that the reversible disaggregation of these Aβ deposits, as well as their irreversible conversion to fibrillar deposits, are similarly stimulated by different apoE isoforms. Deposition of Aβ was associated with increased astrogliosis, both far from and near the Aβ deposits (Fig. 6), suggesting that it might be triggered by both insoluble and soluble Aβ aggregates.

The present finding that i.c.v. infusion of thiorphan induced abundant and widespread deposition of mouse Aβ *in vivo* extends earlier studies in which thiorphan injected directly into the hippocampus induced localized Aβ deposition (26). Preliminary results suggest that i.c.v. infusion of thiorphan into APP-transgenic mice also enhances deposition of human Aβ (data not shown). Aβ deposition in the thiorphan model occurs much more rapidly than that observed in transgenic mice (24, 39). Moreover, the reversibility of Aβ deposition can be more conveniently studied in this

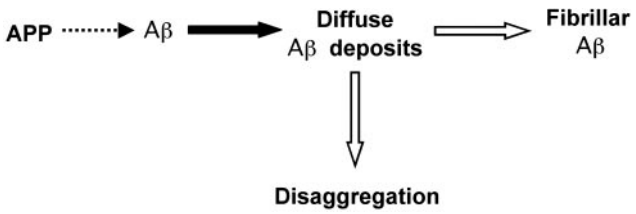

Fig. 7. Schematic presentation of differential and isoform-specific effects of apoE on the deposition, disaggregation, and fibrillization of Aβ. Aggregation of Aβ and formation of immunopositive nonfibrillar (diffuse) deposits (black arrow) are enhanced in an isoform-specific fashion by apoE4, whereas both disaggregation and the fibrillization of these deposits (white arrows) are activated in a similar fashion by different apoE isoforms.

model, probably because after neprilysin is inhibited, there is rapid and reversible accumulation of Aβ, which cannot be readily offset here by mechanisms such as degradation and clearance. This effect renders the thiorphan model uniquely suitable for the study of early and pathologically pertinent stages of the amyloid cascade and for the development of compounds that affect its progression.

Mice deficient in neprilysin, unlike thiorphan-treated mice, do not have Aβ deposits (27). This lack of deposits might be attributable to the presence of neprilysin-like peptidases in the brain that are also sensitive to thiorphan (40) and whose activity is not impaired in neprilysin-deficient mice. Moreover, because neprilysin is externally oriented, the Aβ deposition resulting from thiorphan treatment probably originates extracellularly. This hypothesis also might explain why, after treatment with thiorphan, the increase in Aβ and its subsequent deposition were not prevented by the Aβ-degrading enzyme insulin-degrading enzyme, which is intracellular (28, 41) and insensitive to thiorphan.

The findings that apoE4 stimulates deposition of Aβ and apoE deficiency blocks formation of fibrillar Aβ deposits are in accordance with and extend previous studies with APP × apoE double-transgenic mice and with APP-transgenic mice on a null apoE mouse background (24, 36, 39, 42, 43). Formation of Aβ deposits did not require apoE, but it was accelerated significantly and in an isoform-specific fashion by apoE4 (Figs. 2 and 3). Furthermore, Aβ deposits in apoE-transgenic and control mice all contain apoE (data not shown), suggesting that the isoform-specific effects of apoE4 on Aβ deposition are related to isoform-specific structural features of the apoE4–Aβ complex, which enhance nucleation and deposition of Aβ. Because the size and growth of Aβ deposits were not affected by apoE, we can conclude that growth of these deposits is not greatly affected by this nucleation apoE4–Aβ complex. Furthermore, because the Aβ42 deposits are smaller and more numerous than the Aβ40 deposits (Figs. 1 and 3), and because Aβ40 codeposits with Aβ42 (data not shown), it seems that the specific stimulation of Aβ deposition by apoE4 is mediated by apoE4–Aβ42 nucleation complexes.

Depending on experimental conditions, binding of apoE4 to Aβ *in vitro* is either stronger or weaker than that of apoE3 (44–49). The present results suggest that *in vivo*, apoE4–Aβ complexes are the most effective nucleation centers. This finding might be a direct result of structural differences between apoE3 and apoE4 and the lipoproteins in which they are embedded, but it also might involve a third component (50–52).

Several mechanisms might conceivably explain the non-isoform-specific effects of apoE on disaggregation and dissolution of the Aβ deposits. ApoE, which in the brain is associated with high-density-lipoprotein-like lipoproteins, binds avidly to Aβ (44, 46, 53) and thus can serve as a shuttle that promotes exchanges of Aβ between soluble and deposited pools. Accordingly, conditions that accompany reactivation of neprilysin (relatively small amounts of soluble Aβ and relatively large numbers of insoluble Aβ deposits) will favor transfer of Aβ by apoE from the soluble to the insoluble pool. Because Aβ deposits of all mouse groups, except for apoE-deficient mice, contain apoE, it is also possible that apoE destabilizes the outer surface of the Aβ deposits. The ratio of fibrillar to nonfibrillar Aβ deposits was similar in all apoE-containing groups (Fig. 3). This finding is in accordance with the notion that fibrillar deposits evolve from diffuse Aβ deposits and that stimulation of fibrillization by apoE is a consequence of its effects on intrinsic properties of the Aβ deposits. Taken together, our present findings suggest that nucleation of Aβ deposition is enhanced in an isoform-specific fashion by apoE4; that apoE does not significantly affect growth of the Aβ deposits; and that both disaggregation of these deposits and their irreversible conversion to fibrillar Aβ are accelerated, although not in an isoform-specific fashion, by apoE.

Converging evidence suggests that both insoluble oligomers and soluble Aβ deposits are pathological and that the effects of Aβ in AD are mediated by early events in the Aβ aggregation cascade.

The present findings in an animal model that apoE4 stimulates the Aβ cascade and that such stimulation is associated with astrogliosis suggest that the increased amyloid load observed in apoE4-positive AD patients reflects early and pathologically important interactions between Aβ and apoE4. Future studies of the correlation between the extent of Aβ aggregation after inhibition of neprilysin and the temporal and spatial distribution of the associated brain pathology can be expected to facilitate evaluation of the relative pathological effects of distinct soluble Aβ oligomers and insoluble polymeric aggregates.

We thank Dr. Allen Roses (Duke University, Durham, NC) and Glaxo Wellcome for kindly providing the transgenic mice; Dr. T. Hartmann for the many fruitful discussions; and Ms. Shirley Smith and Ms. Angela Cohen for editorial assistance. mAbs G210 and G211 were kindly provided by Dr. T. Hartmann, and antisera FC35420 and FC3340 were a generous gift from Dr. F. Checler. This work was supported in part by European Community Grant QLK-2002-172 LIPIDIET (to D.M.M.), Israel Academy of Sciences and Humanities Grant 43/00-1, and grants from the Harry Stern National Center for Alzheimer's Disease and the Eichenbaum Foundation. D.M.M. is the incumbent of the Myriam Lebach Chair in Molecular Neurodegeneration (Tel Aviv University).

1. Hardy, J. & Selkoe, D. J. (2002) *Science* **297,** 353–356.
2. Selkoe, D. J. (2001) *Physiol. Rev.* **81,** 741–766.
3. Roher, A. E., Chaney, M. O., Kuo, Y. M., Webster, S. D., Stine, W. B., Haverkamp, L. J., Woods, A. S., Cotter, R. J., Tuohy, J. M., Krafft, G. A., *et al.* (1996) *J. Biol. Chem.* **271,** 20631–20635.
4. Lambert, M. P., Barlow, A. K., Chromy, B. A., Edwards, C., Freed, R., Liosatos, M., Morgan, T. E., Rozovsky, I., Trommer, B., Viola, K. L., *et al.* (1998) *Proc. Natl. Acad. Sci. USA* **95,** 6448–6453.
5. Hartley, D. M., Walsh, D. M., Ye, C. P., Diehl, T., Vasquez, S., Vassilev, P. M., Teplow, D. B. & Selkoe, D. J. (1999) *J. Neurosci.* **19,** 8876–8884.
6. Walsh, D. M., Hartley, D. M., Kusumoto, Y., Fezoui, Y., Condron, M. M., Lomakin, A., Benedek, G. B., Selkoe, D. J. & Teplow, D. B. (1999) *J. Biol. Chem.* **274,** 25945–25952.
7. Walsh, D. M., Klyubin, I., Fadeeva, J. V., Cullen, W. K., Anwyl, R., Wolfe, M. S., Rowan, M. J. & Selkoe, D. J. (2002) *Nature* **416,** 535–539.
8. Ward, R. V., Jennings, K. H., Jepras, R., Neville, W., Owen, D. E., Hawkins, J., Christie, G., Davis, J. B., George, A., Karran, E. H., *et al.* (2000) *Biochem. J.* **348,** 137–144.
9. Oddo, S., Caccamo, A., Shepherd, J. D., Murphy, M. P., Golde, T. E., Kayed, R., Metherate, R., Mattson, M. P., Akbari, Y. & LaFerla, F. M. (2003) *Neuron* **39,** 409–421.
10. Gong, Y., Chang, L., Viola, K. L., Lacor, P. N., Lambert, M. P., Finch, C. E., Krafft, G. A. & Klein, W. L. (2003) *Proc. Natl. Acad. Sci. USA* **100,** 10417–10422.
11. Terry, R. D., Peck, A., DeTeresa, R., Schechter, R. & Horoupian, D. S. (1981) *Ann. Neurol.* **10,** 184–192.
12. Braak, H. & Braak, E. (1991) *Acta Neuropathol.* **82,** 239–259.
13. Dickson, D. W., Crystal, H. A., Bevona, C., Honer, W., Vincent, I. & Davies, P. (1995) *Neurobiol. Aging* **16,** 285–298; discussion 298–304.
14. Hsia, A. Y., Masliah, E., McConlogue, L., Yu, G. Q., Tatsuno, G., Hu, K., Kholodenko, D., Malenka, R. C., Nicoll, R. A. & Mucke, L. (1999) *Proc. Natl. Acad. Sci. USA* **96,** 3228–3233.
15. Dodart, J. C., Mathis, C., Bales, K. R., Paul, S. M. & Ungerer, A. (1999) *Neurosci. Lett.* **277,** 49–52.
16. Lee, K. W., Lee, S. H., Kim, H., Song, J. S., Yang, S. D., Paik, S. G. & Han, P. L. (2004) *J. Neurosci. Res.* **76,** 572–580.
17. Mahley, R. W. & Rall, S. C., Jr. (2000) *Annu. Rev. Genomics Hum. Genet.* **1,** 507–537.
18. Corder, E. H., Saunders, A. M., Strittmatter, W. J., Schmechel, D. E., Gaskell, P. C., Small, G. W., Roses, A. D., Haines, J. L. & Pericak-Vance, M. A. (1993) *Science* **261,** 921–923.
19. Saunders, A. M., Strittmatter, W. J., Schmechel, D., St. George-Hyslop, P. H., Pericak-Vance, M. A., Joo, S. H., Rosi, B. L., Gusella, J. F., Crapper-MacLachlan, D. R., Alberts, M. J., *et al.* (1993) *Neurology* **43,** 1467–1472.
20. Roses, A. D. (1996) *Annu. Rev. Med.* **47,** 387–400.
21. Schmechel, D. E., Saunders, A. M., Strittmatter, W. J., Crain, B. J., Hulette, C. M., Joo, S. H., Pericak-Vance, M. A., Goldgaber, D. & Roses, A. D. (1993) *Proc. Natl. Acad. Sci. USA* **90,** 9649–9653.
22. Bales, K. R., Verina, T., Dodel, R. C., Du, Y., Altstiel, L., Bender, M., Hyslop, P., Johnstone, E. M., Little, S. P., Cummins, D. J., *et al.* (1997) *Nat. Genet.* **17,** 263–264.
23. Holtzman, D. M., Bales, K. R., Wu, S., Bhat, P., Parsadanian, M., Fagan, A. M., Chang, L. K., Sun, Y. & Paul, S. M. (1999) *J. Clin. Invest.* **103,** R15–R21.
24. Holtzman, D. M., Bales, K. R., Tenkova, T., Fagan, A. M., Parsadanian, M., Sartorius, L. J., Mackey, B., Olney, J., McKeel, D., Wozniak, D., *et al.* (2000) *Proc. Natl. Acad. Sci. USA* **97,** 2892–2897.
25. Brendza, R. P., Bales, K. R., Paul, S. M. & Holtzman, D. M. (2002) *Mol. Psychiatry* **7,** 132–135.
26. Iwata, N., Tsubuki, S., Takaki, Y., Watanabe, K., Sekiguchi, M., Hosoki, E., Kawashima-Morishima, M., Lee, H. J., Hama, E., Sekine-Aizawa, Y., *et al.* (2000) *Nat. Med.* **6,** 143–150.
27. Iwata, N., Tsubuki, S., Takaki, Y., Shirotani, K., Lu, B., Gerard, N. P., Gerard, C., Hama, E., Lee, H. J. & Saido, T. C. (2001) *Science* **292,** 1550–1552.
28. Farris, W., Mansourian, S., Chang, Y., Lindsley, L., Eckman, E. A., Frosch, M. P., Eckman, C. B., Tanzi, R. E., Selkoe, D. J. & Guenette, S. (2003) *Proc. Natl. Acad. Sci. USA* **100,** 4162–4167.
29. Eckman, E. A., Watson, M., Marlow, L., Sambamurti, K. & Eckman, C. B. (2003) *J. Biol. Chem.* **278,** 2081–2084.
30. Leissring, M. A., Farris, W., Chang, A. Y., Walsh, D. M., Wu, X., Sun, X., Frosch, M. P. & Selkoe, D. J. (2003) *Neuron* **40,** 1087–1093.
31. Marr, R. A., Rockenstein, E., Mukherjee, A., Kindy, M. S., Hersh, L. B., Gage, F. H., Verma, I. M. & Masliah, E. (2003) *J. Neurosci.* **23,** 1992–1996.
32. Xu, P. T., Schmechel, D., Rothrock-Christian, T., Burkhart, D. S., Qiu, H. L., Popko, B., Sullivan, P., Maeda, N., Saunders, A. M., Roses, A. D., *et al.* (1996) *Neurobiol. Dis.* **3,** 229–245.
33. Levi, O., Jongen-Relo, A. L., Feldon, J., Roses, A. D. & Michaelson, D. M. (2003) *Neurobiol. Dis.* **13,** 273–282.
34. Ophir, G., Meilin, S., Efrati, M., Chapman, J., Karussis, D., Roses, A. & Michaelson, D. M. (2003) *Neurobiol. Dis.* **12,** 56–64.
35. Sabo, T., Lomnitski, L., Nyska, A., Beni, S., Maronpot, R. R., Shohami, E., Roses, A. D. & Michaelson, D. M. (2000) *Neuroscience* **101,** 879–884.
36. Ida, N., Hartmann, T., Pantel, J., Schroder, J., Zerfass, R., Forstl, H., Sandbrink, R., Masters, C. L. & Beyreuther, K. (1996) *J. Biol. Chem.* **271,** 22908–22914.
37. Fagan, A. M., Watson, M., Parsadanian, M., Bales, K. R., Paul, S. M. & Holtzman, D. M. (2002) *Neurobiol. Dis.* **9,** 305–318.
38. Paxinos, G. & Franklin, K. B. J. (1997) *The Mouse Brain in Stereotaxic Coordinates* (Academic, Orlando, FL).
39. Buttini, M., Yu, G. Q., Shockley, K., Huang, Y., Jones, B., Masliah, E., Mallory, M., Yeo, T., Longo, F. M. & Mucke, L. (2002) *J. Neurosci.* **22,** 10539–10548.
40. Shirotani, K., Tsubuki, S., Iwata, N., Takaki, Y., Harigaya, W., Maruyama, K., Kiryu-Seo, S., Kiyama, H., Iwata, H., Tomita, T., *et al.* (2001) *J. Biol. Chem.* **276,** 21895–21901.
41. Edbauer, D., Willem, M., Lammich, S., Steiner, H. & Haass, C. (2002) *J. Biol. Chem.* **277,** 13389–13393.
42. Bales, K. R., Verina, T., Cummins, D. J., Du, Y., Dodel, R. C., Saura, J., Fishman, C. E., DeLong, C. A., Piccardo, P., Petegnief, V., *et al.* (1999) *Proc. Natl. Acad. Sci. USA* **96,** 15233–15238.
43. Carter, D. B., Dunn, E., McKinley, D. D., Stratman, N. C., Boyle, T. P., Kuiper, S. L., Oostveen, J. A., Weaver, R. J., Boller, J. A. & Gurney, M. E. (2001) *Ann. Neurol.* **50,** 468–475.
44. Strittmatter, W. J., Weisgraber, K. H., Huang, D. Y., Dong, L. M., Salvesen, G. S., Pericak-Vance, M., Schmechel, D., Saunders, A. M., Goldgaber, D. & Roses, A. D. (1993) *Proc. Natl. Acad. Sci. USA* **90,** 8098–8102.
45. Strittmatter, W. J. & Roses, A. D. (1996) *Annu. Rev. Neurosci.* **19,** 53–77.
46. LaDu, M. J., Falduto, M. T., Manelli, A. M., Reardon, C. A., Getz, G. S. & Frail, D. E. (1994) *J. Biol. Chem.* **269,** 23403–23406.
47. Evans, K. C., Berger, E. P., Cho, C. G., Weisgraber, K. H. & Lansbury, P. T., Jr. (1995) *Proc. Natl. Acad. Sci. USA* **92,** 763–767.
48. Wisniewski, T., Ghiso, J. & Frangione, B. (1997) *Neurobiol. Dis.* **4,** 313–328.
49. Tokuda, T., Calero, M., Matsubara, E., Vidal, R., Kumar, A., Permanne, B., Zlokovic, B., Smith, J. D., Ladu, M. J., Rostagno, A., *et al.* (2000) *Biochem. J.* **348,** 359–365.
50. Atwood, C. S., Moir, R. D., Huang, X., Scarpa, R. C., Bacarra, N. M., Romano, D. M., Hartshorn, M. A., Tanzi, R. E. & Bush, A. I. (1998) *J. Biol. Chem.* **273,** 12817–12826.
51. Fagan, A. M., Holtzman, D. M., Munson, G., Mathur, T., Schneider, D., Chang, L. K., Getz, G. S., Reardon, C. A., Lukens, J., Shah, J. A. & LaDu, M. J. (1999) *J. Biol. Chem.* **274,** 30001–30007.
52. Yamauchi, K., Tozuka, M., Hidaka, H., Hidaka, E., Kondo, Y. & Katsuyama, T. (1999) *Clin. Chem.* **45,** 1431–1438.
53. Wisniewski, T., Golabek, A., Matsubara, E., Ghiso, J. & Frangione, B. (1993) *Biochem. Biophys. Res. Commun.* **192,** 359–365.